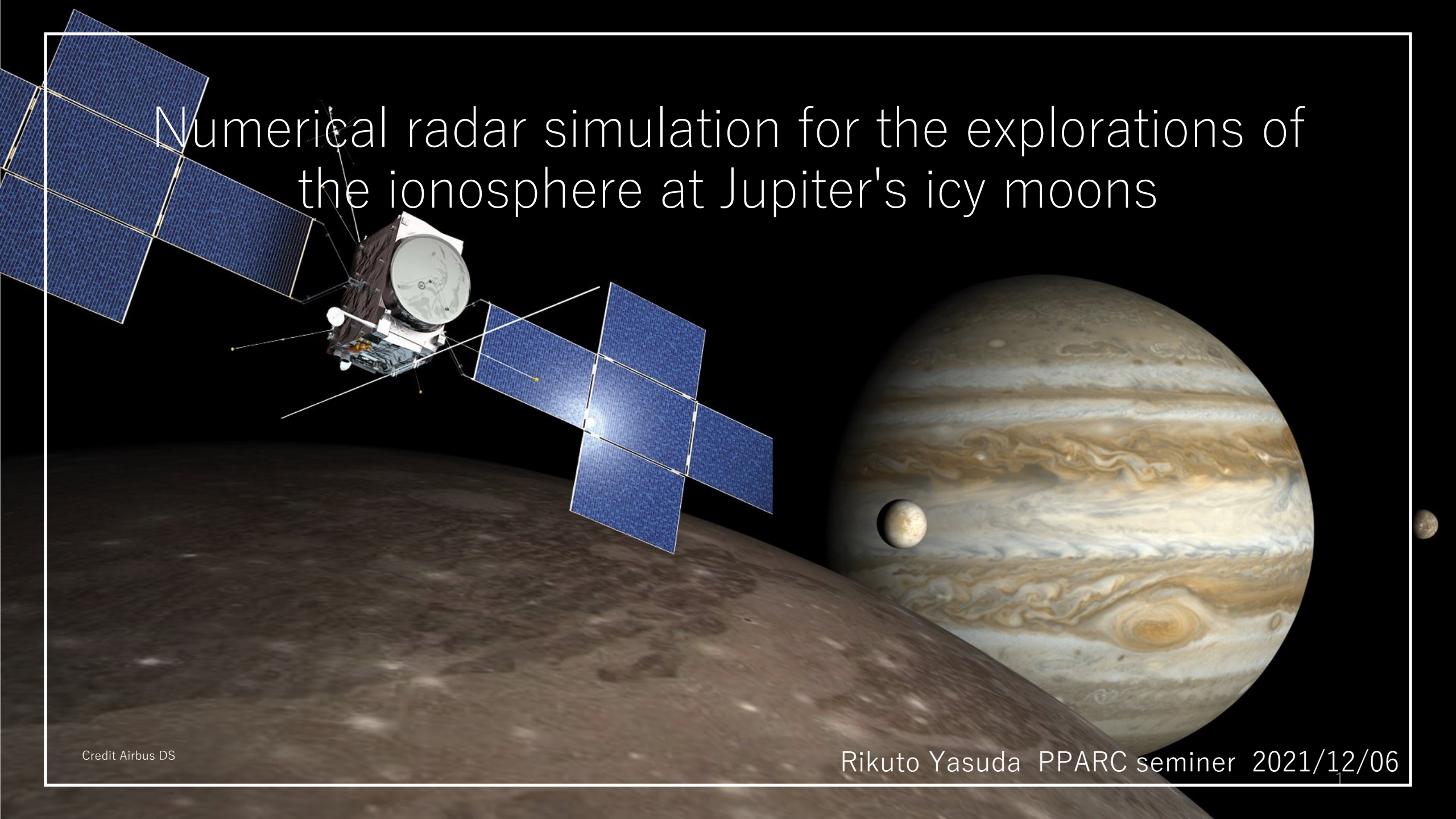


# Numerical radar simulation for the explorations of the ionosphere at Jupiter's icy moons



## 1. Introduction

- 1-1. Jupiter's icy moon
- 1-2 Radio observation at Jupiter's icy moon
- 1-3 Previous observation of moon's ionosphere
- 1-4 Preceding studies of Jovian radio emission occultations
- 1-5 Purpose of this study

## 4. Conclusion

## 5. Future works

Reference  
Appendix

## 2. Method

- 2-1 How to combine Raytracing method  
with Radio Emission Simulations
- 2-2 Raytracing
- 2-3 Verify time-step validity of raytracing code

## 3. Radio occultation observation

- 3-1 Ganymede ionosphere model
- 3-2 Ganymede ionosphere result
- 3-3 Discussion

# 1-1. Jupiter's icy moon

~ Jupiter's icy moon ~

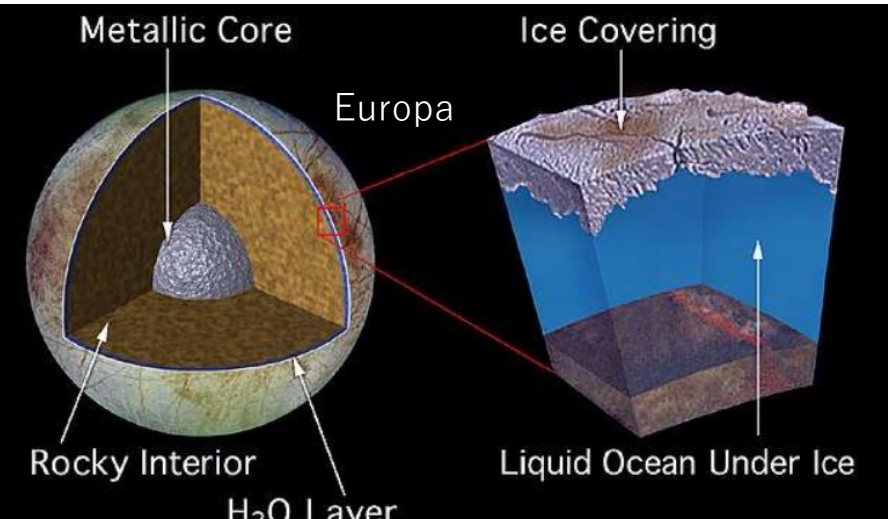
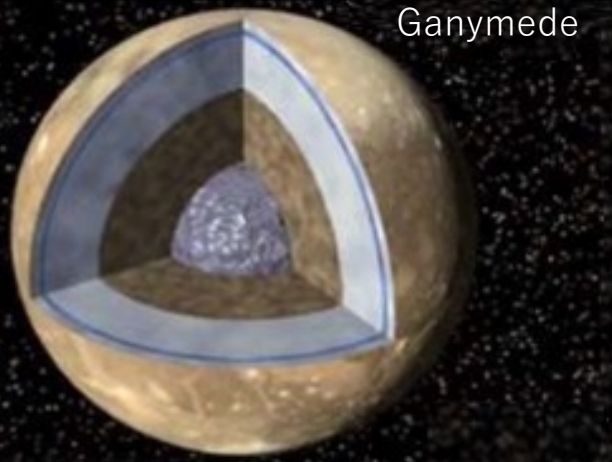


Fig.1 Model interiors of Ganymede and Europa [ Schubert et al, 2004]

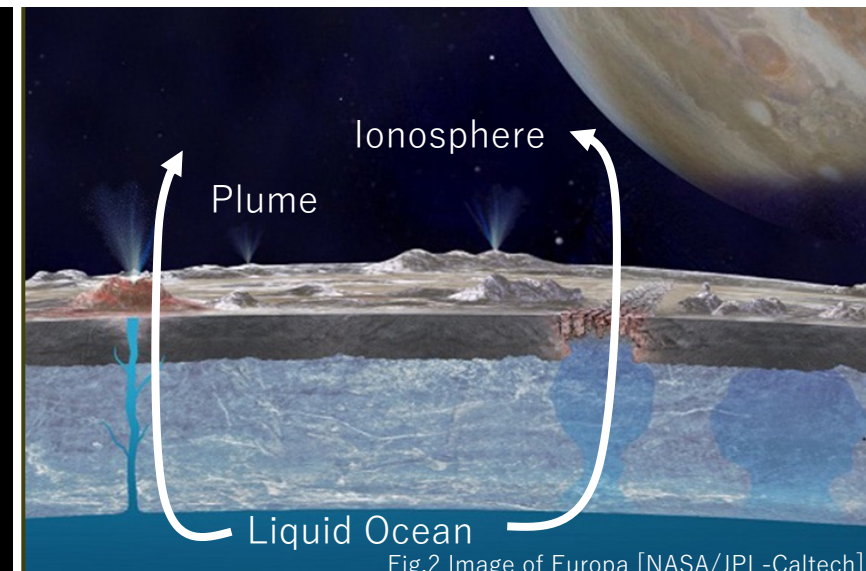


Fig.2 Image of Europa [NASA/JPL-Caltech]

## Jupiter's icy moon (ex. Europa, Ganymede)

- possess internal liquid-water oceans [Khurana et al., 1998; Kivelson et al., 2002 etc..]
- Multiple icy bodies have subsurface ocean while only Earth has surface ocean.

Structures of the interior, ionosphere and plume of the icy moons are essential information for understanding universality of habitable environment.

It is impossible to observe directly ionosphere and plumes at low altitude as well as interiors.

# 1-2. Radio observation at Jupiter's icy moon

4

## JUICE (JUpiter ICy moons Explorer)

### Radio and Plasma Wave Investigation (RPWI) [Frequency: 80kHz~45MHz]

- ... A radio plasma wave instrument to characterize radio emission and plasma environment
- Apply to radio occultation observation or passive radar. (Fig.4, 5)



Fig.3 JUICE [Airbus DS]

#### ① Radio occultation observation

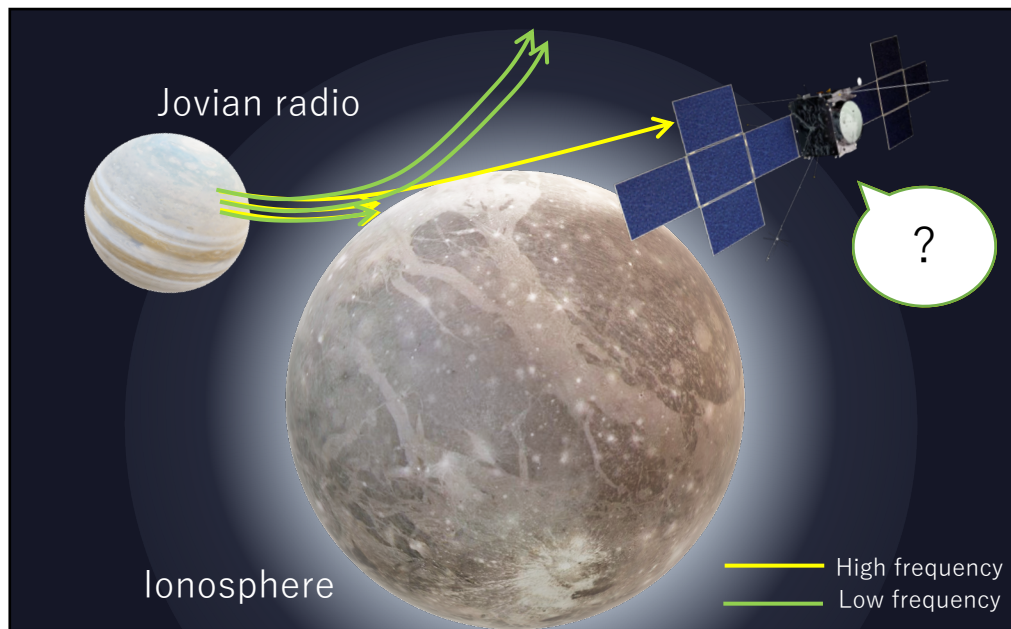


Fig.4 Radio observation using Jovian radio refraction  
(adapted from Airbus DS and NASA/JPL)

#### ② Passive radar

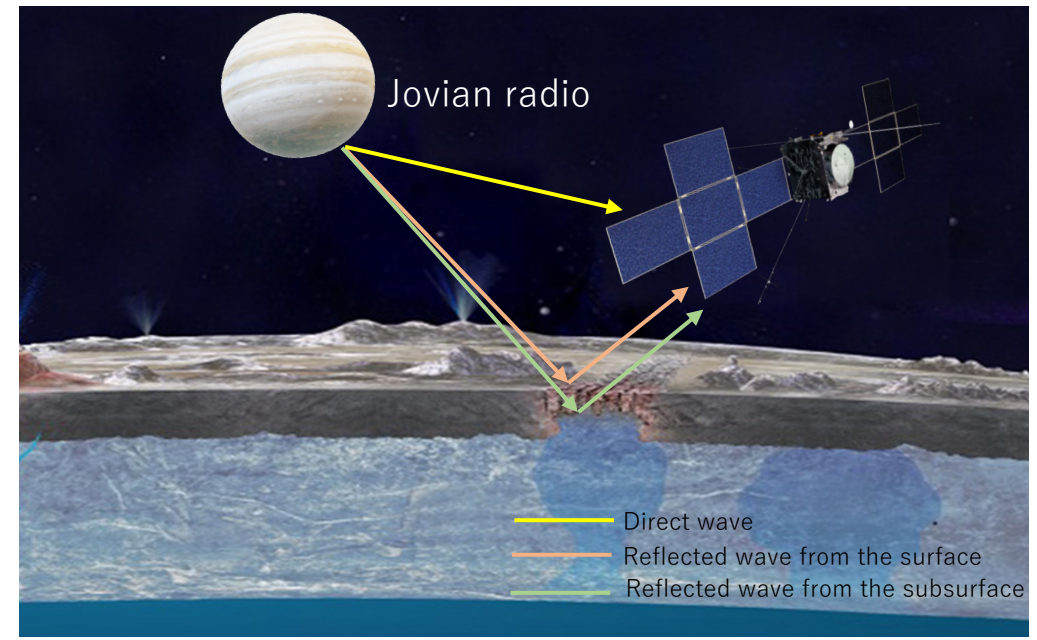


Fig.5 Radio observation using Jovian radio reflection  
(adapted from NASA/JPL, Airbus DS and gcoe-earths.org)

# 1-3. Previous observation of moon's ionosphere

5

## Ganymede ionosphere

- In-situ observation [Galileo PWS] (Fig.6)

Maximum ion densities

… ~200/cc (altitude:200km)

[Eviatar et al. 2001]

Lack of information at low altitude

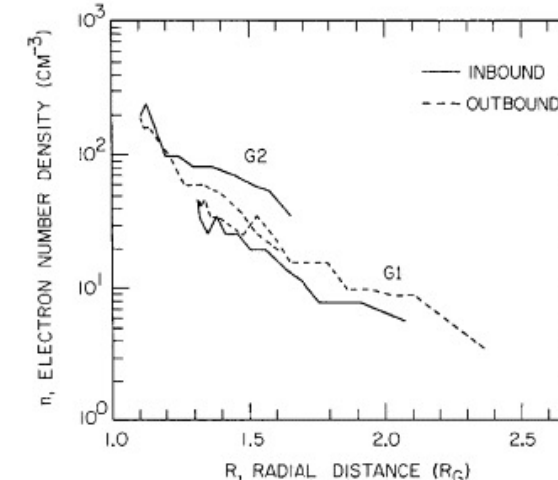


Fig.6 Electron density profiles on Ganymede 2 obtained by means of the PWS instrument on Galileo [Eviatar et al, 2001]

- Radio occultation [Galileo] (Fig.7&8)

6 measurements provided inconclusive results in 4 instances

Maximum electron densities … ~5000/cc

[Kliore et al, 2001b]

Only ionosphere around day-night boundary

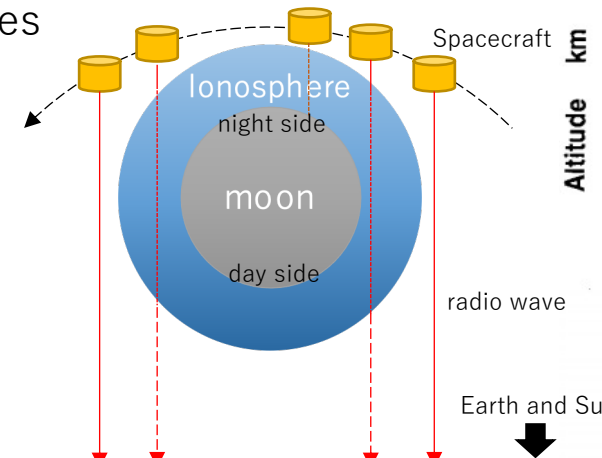


Fig.7 Radio observation using Jovian radio ref

→ limited observations!!

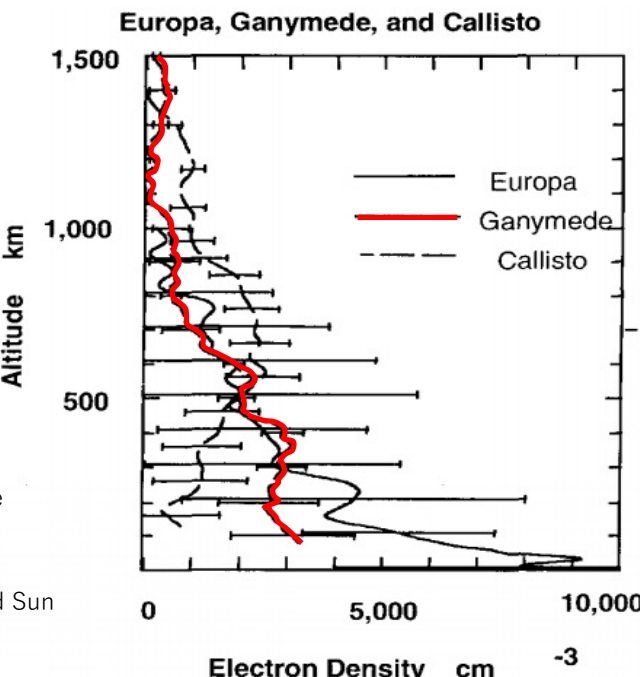


Fig.8 Averaged electron density profiles for Europa, Ganymede and Calisto. [Kliore et al, 1998]

## Occultation modeling using ExPRES Jovian Radio Emission Simulations [Cecconi et al, 2021]

※ Assuming a straight-line propagation (no refraction)

- At lower frequencies, the occultation spectral egress occurs later than predicted. (Fig. 10)
- This prediction mismatch indicates that propagation effects play an important role in the fine understanding of the radio occultation near Galilean moons.

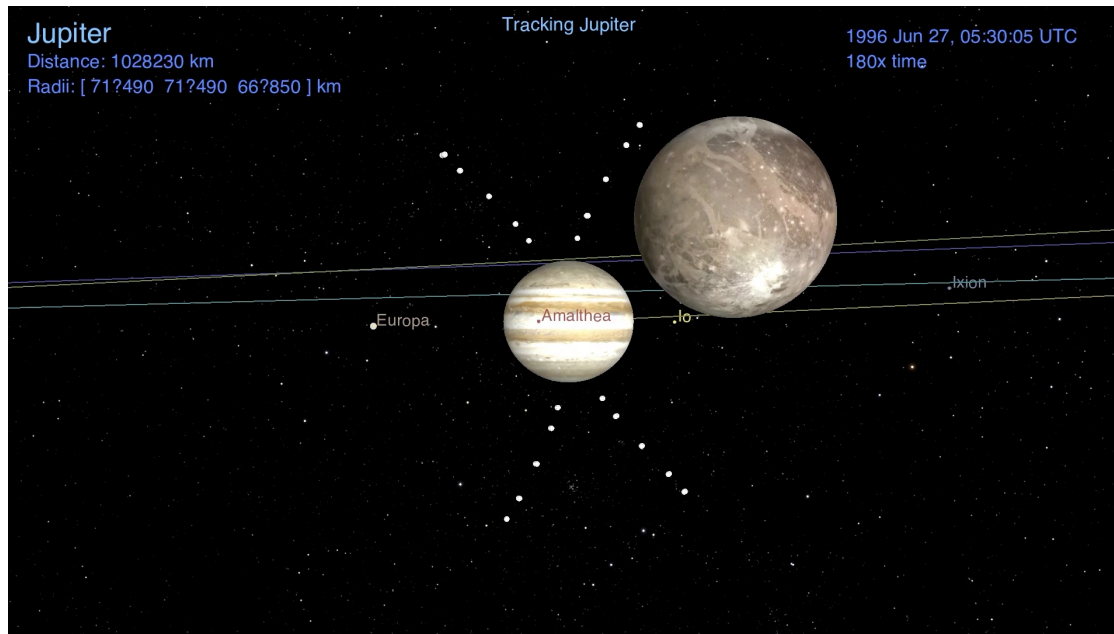


Fig.9 Flyby visualized in the Cosmographia tool. The scene is set with an observer on the Galileo spacecraft, pointing to Jupiter. Ganymede is in the field of view. The ExPRES-modelled visible radio sources are also shown, at 700 kHz, 1 MHz, 2 MHz, 5 MHz and 10 MHz as white dots. The radio sources are conventionally grouped in four sets (named A, B, C and D). [Cecconi et al, 2021]

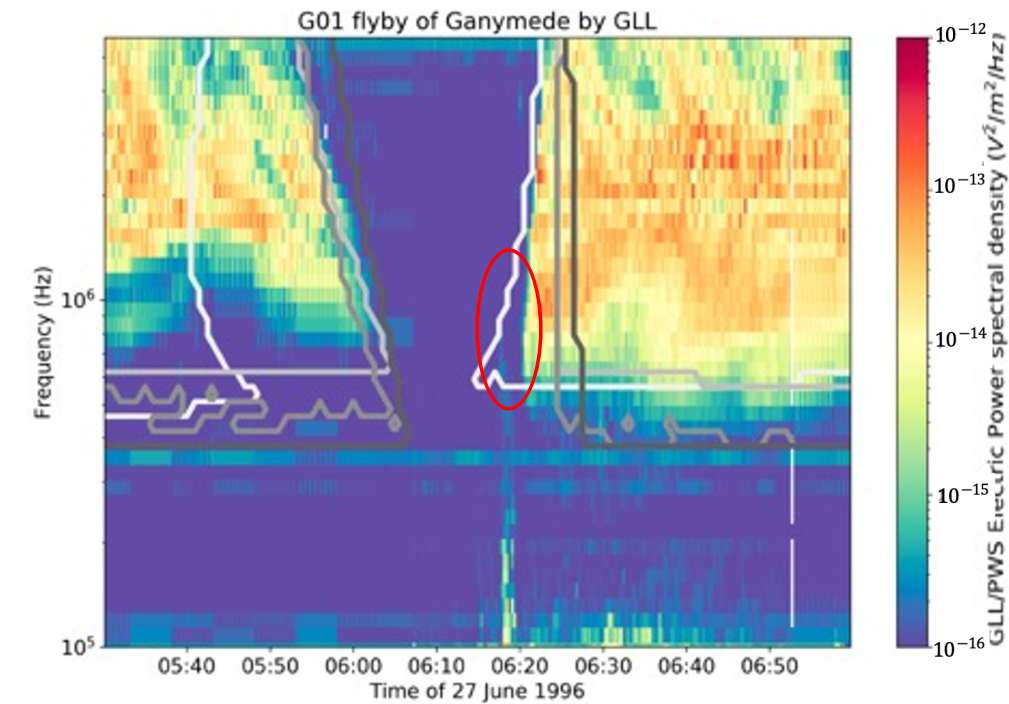


Fig.10 Superimposed Galileo PWS data and ExPRES simulations during Jovian radio emission occultations by Ganymede . The four types of emission (A, B, C, D) are separated (from white to darkgrey, resp.) [Cecconi et al, 2021]

# 1-5. Purpose of this study

7

- To investigate spatial structures of ionosphere and plumes created from the water oceanic materials, developing the numerical simulation code for the radar explorations using natural radio waves. [Fig. 4]  
(Collaborative research with institutions in France and Sweden)
- Finally, we will also investigate spatial structures of the interior. [Fig. 5]



① Radio occultation observation

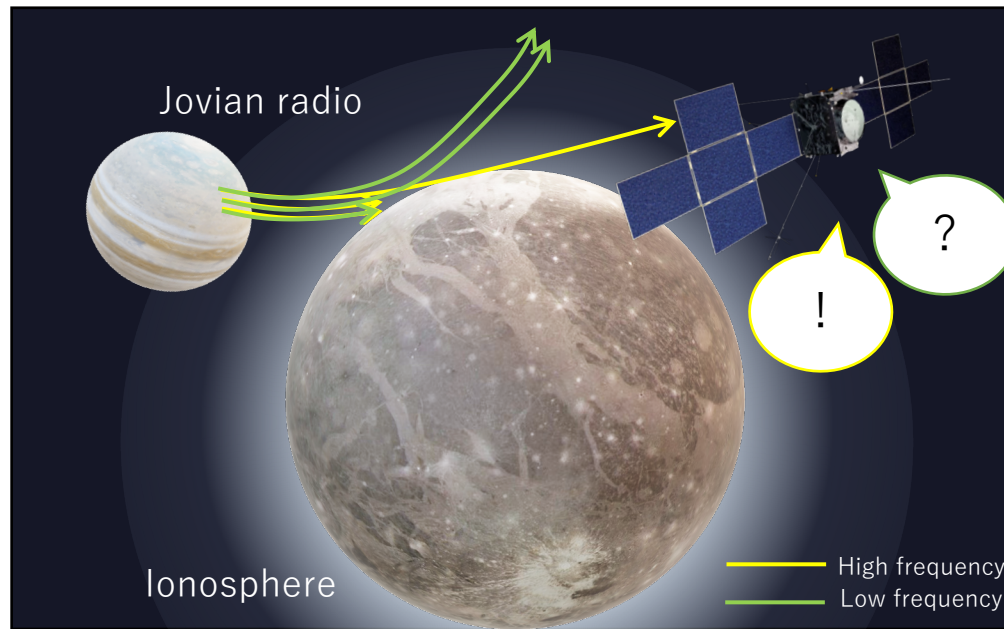


Fig.4 Radio observation using Jovian radio refraction (adapted from Airbus DS and NASA/JPL)

② Passive radar

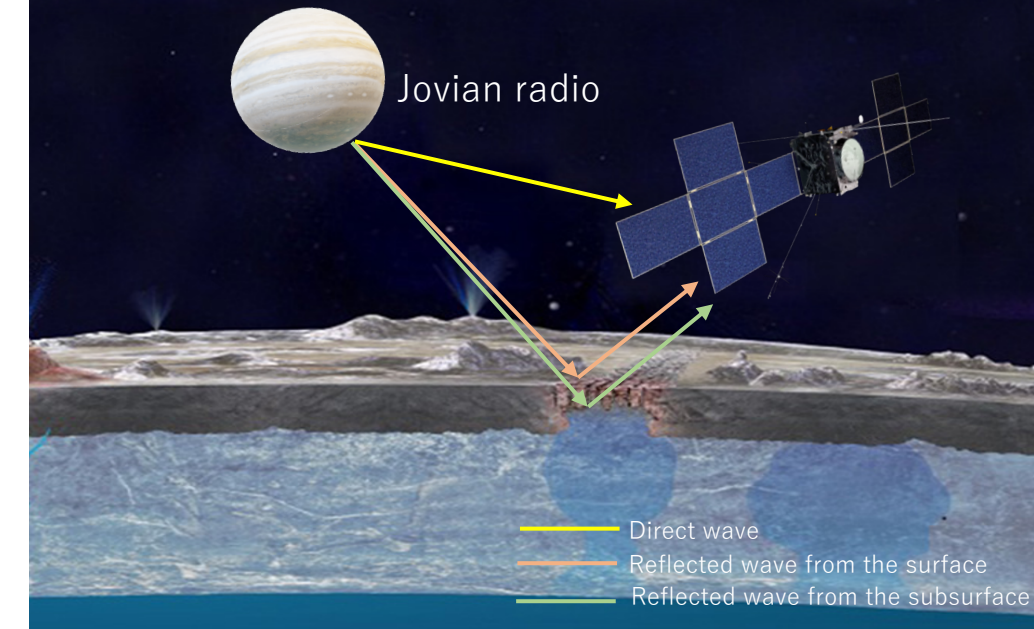


Fig.5 Radio observation using Jovian radio reflection (adapted from NASA/JPL, Airbus DS and gcoe-earths.org)

Today's topic..

- Emulate occultation of the Jovian radio waves during the flybys of the Galileo spacecraft to Ganymede including the ionospheric refraction effect
- Propose the vertical ionospheric profiles at the altitude below the orbiter

## ExPRES Jovian Radio Emission Simulations

Ephemeris of the observer



The position of the radio sources (➡ in Fig.8)  
 (The radio is emitted in the direction of the observer)

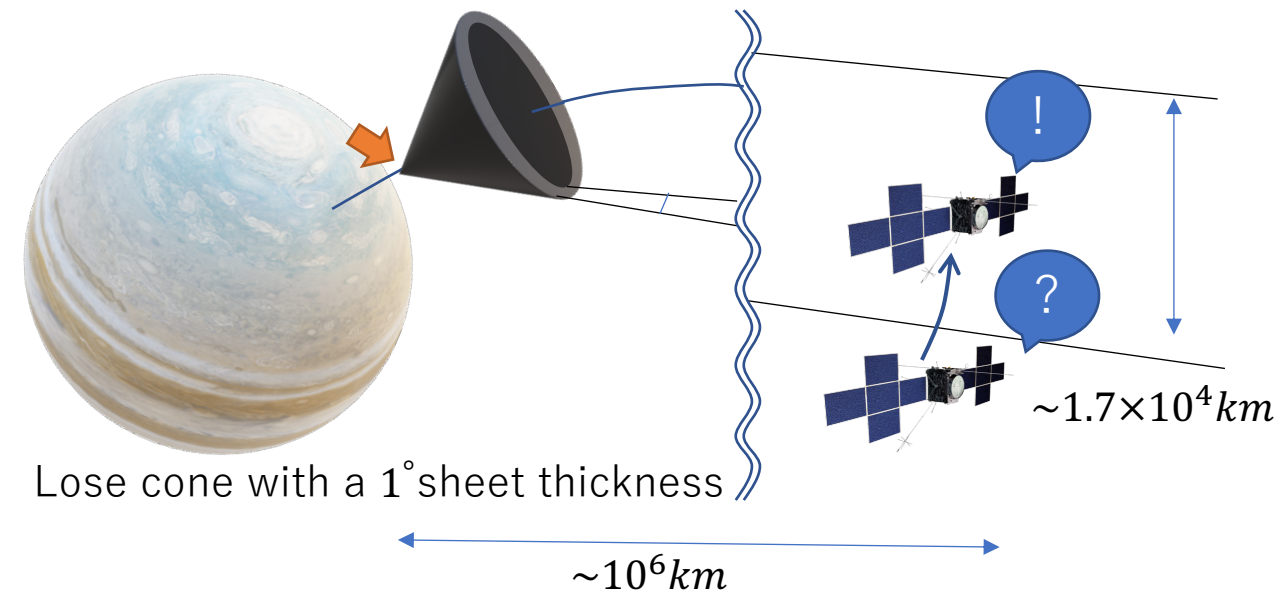


Fig.11 The position of the radio source and the direction of the radio emission  
 (adapted from Airbus DS and NASA/JPL)

## To simulate refraction of Jovian radio waves

Assuming the radio waves are ..

- plane waves
- having -3000km width
- refracting only in the ionosphere of Ganymede

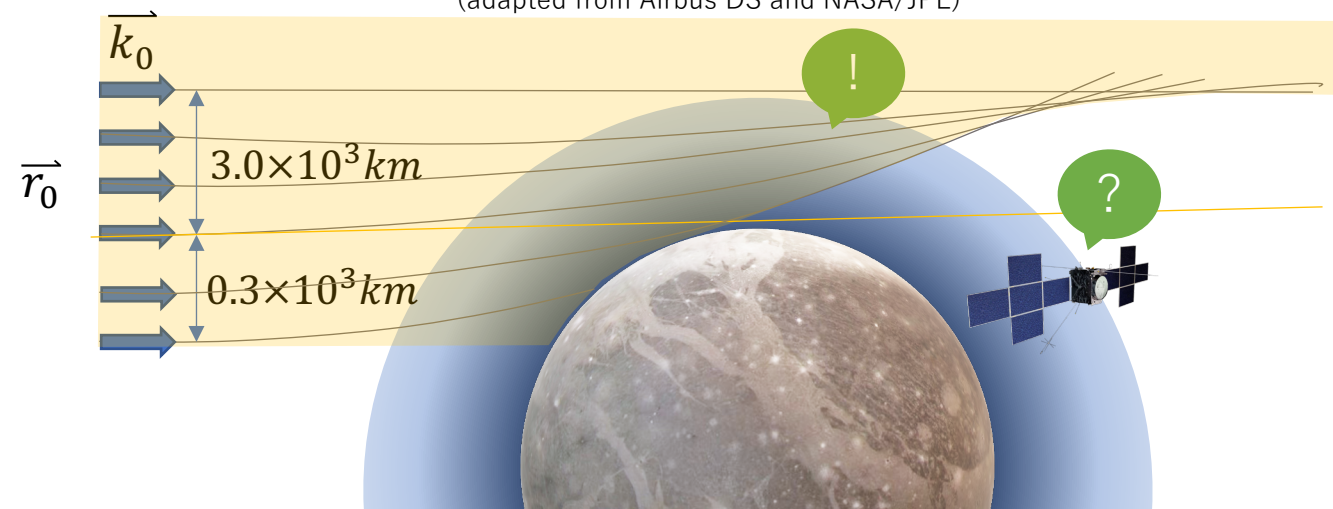


Fig.12 Initial positions ( $\vec{r}_0$ ) and Initial wave vectors ( $\vec{k}_0$ ) of the radio waves in our raytracing code

- In numerical radar simulation, full wave simulation is general method.

ex) FDTD (Finite-difference time-domain method) method (Fig.13)  
 ...Solving Maxwell's equations on a mesh and computing E and H at grid points spaced  $\Delta x$ ,  $\Delta y$ , and  $\Delta z$  apart.

- However, this method needs high calculation cost when we execute the program in a wide calculation space such as ionosphere, plumes and interiors of icy moons.

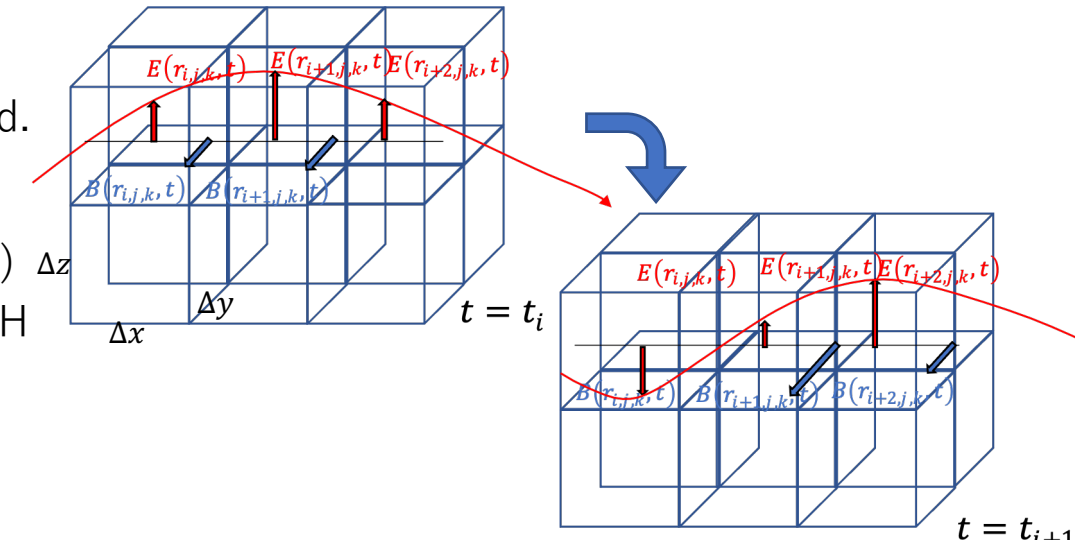


Fig.13 FTDT image

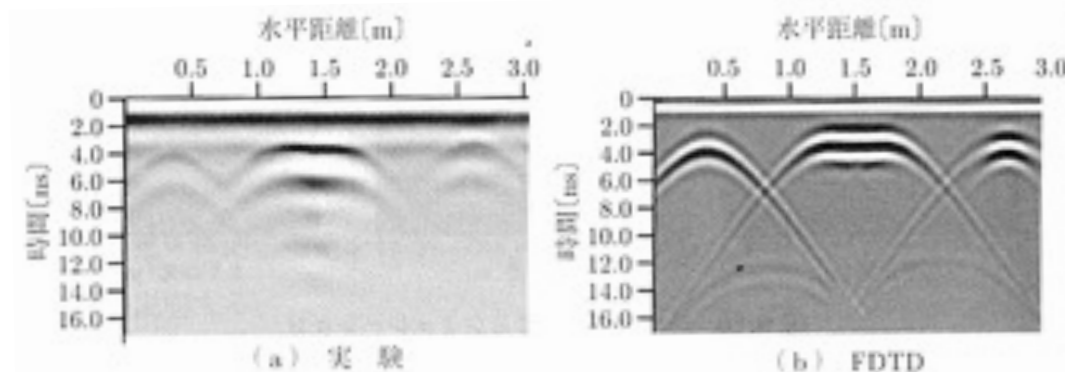


Fig.14 FTDT result [Principles of radar (Kazuo Ouchi)]

### Ray tracing ..

more computationally efficient to trace propagation paths of electromagnetic waves in the magnetized plasma, sequentially solving the dispersion relation for plasma waves.

~ input parameter ~

- Magnetic field model  $\omega_c(\vec{r}, t)$
- Plasma density model  $\omega_p(\vec{r}, t)$
- Frequency of wave ( $\omega$ )
- Initial position ( $\vec{r}_0$ )
- Initial wave vector ( $\vec{k}_0$ )



$d\vec{r}_{j+1}$  and  $d\vec{k}_{j+1}$  in  $dt_j$

$$(1) \rightarrow d\vec{r}_{j+1} = -\frac{\partial D_j / \partial \vec{k}_j}{\partial D_j / \partial \omega} \cdot dt_j, \quad d\vec{k}_{j+1} = +\frac{\partial D_j / \partial \vec{r}_j}{\partial D_j / \partial \omega} \cdot dt_j$$



the time ( $t_{j+1}$ ), position ( $\vec{r}_{j+1}$ ) and wave vector ( $\vec{k}_{j+1}$ ) after  $dt_j$

- $t_{j+1} = t_j + dt_j$
- $\vec{r}_{j+1} = \vec{r}_j + d\vec{r}_{j+1}$
- $\vec{k}_{j+1} = \vec{k}_j + d\vec{k}_{j+1}$



~ output ~

a full ray path and time ( $\vec{r}(t)$ )

- Equation of motion of plasma

$$\frac{d\vec{v}}{dx} = \frac{q}{m} (\vec{E} + \vec{v} \times \vec{B})$$

- Maxwell's equations

$$\nabla \times \vec{H} = \vec{j} + \frac{\partial \vec{D}}{\partial t} \quad \nabla \times \vec{E} = -\frac{\partial \vec{B}}{\partial t}$$



(Cold plasma · Discarding plasma collision)

Appleton-Hartree equation (Cf. Appendix A)

~The dispersion relation of waves in magnetized cold plasma~

$$D(t, \vec{r}, \omega, \vec{k}) = \left( \frac{c|\vec{k}|}{\omega} \right)^2 + \frac{2X}{2 - \frac{Y^2 \sin^2 \theta}{1-X} + \rho \sqrt{\frac{Y^2 \sin^4 \theta}{(1-X)^2} + 4Y^2 \cos^2 \theta}} - 1 = 0 \quad \dots (1)$$

$$X = \left( \frac{\omega_p}{\omega} \right)^2 \quad Y = \frac{\omega_c}{\omega} \quad \rho = \text{LO mode : 1, RX mode : -1}$$

$\vec{r}, t$  : position of a ray path and time

$\theta$  : an angle between wave normal vector and the local magnetic field vector

$\omega_p$  : plasma frequency (depending on plasma density)

$\omega_c$  : cyclotron frequency (depending on magnetic field)

# 3-1. Ganymede ionosphere model

13

## ~Ganymede ionosphere model~

Plasma density model (Fig.10)

... Hydrostatic equilibrium plasma

$$\text{Max density} : 400 \cdot 200 \cdot 100 \cdot 50 \cdot 25 \cdot 12.5 \text{ (/cc)}$$

$$\text{Scale height} : 900 \cdot 600 \cdot 300 \cdot 150 \text{ (km)}$$

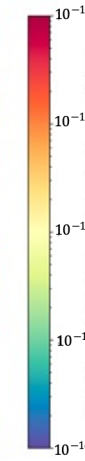
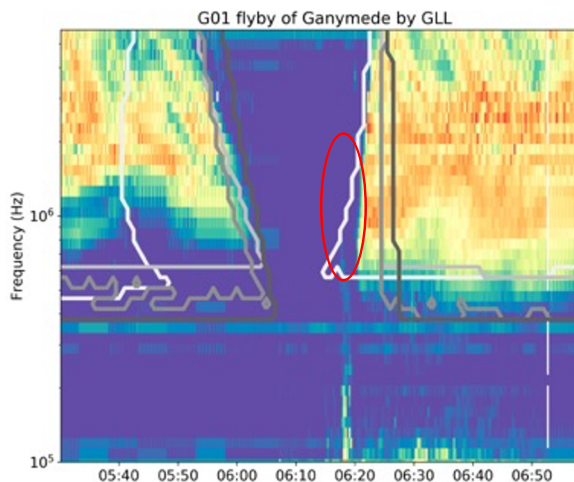
Magnetic field model

... Almost zero magnetic field

$$(1.0 \times 10^{-11} \text{ (T)} \cdot x\text{-axis direction} \cdot \text{uniformly})$$

※  $f_c < f$  at Ganymede surface

( $f_c$  ... Cyclotron frequency,  $f$  ... Frequency of waves)



Simulate f-t diagram assuming multiple hydrostatic equilibrium plasma model  
→ Comparing with Galileo PWS data, we estimate structures of Ganymede ionosphere

Fig.10 Superimposed Galileo PWS data and ExPRES simulations during Jovian radio emission occultations by Ganymede. The four types of emission (A, B, C, D) are separated (from white to darkgrey, resp.) [Cecconi et al, 2021]

## 3-2. Ganymede ionosphere result

14

### Focus on ingress

#### No refraction

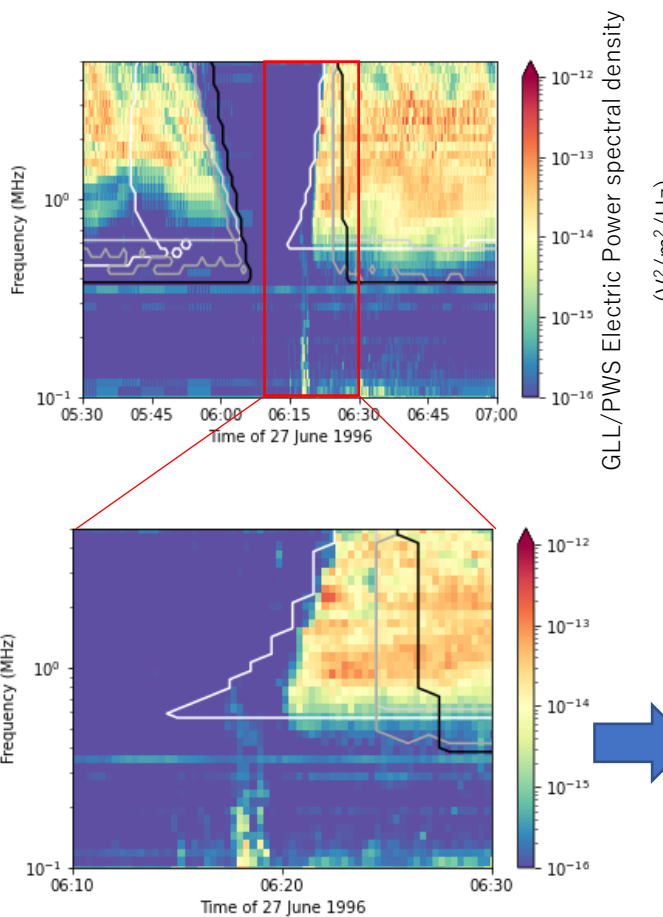


Fig.16 Superimposed Galileo PWS data and ExPRES simulations during Jovian radio emission occultations' egress by Ganymede . The four types of emission (A, B, C, D) are separated (from white to darkgrey, resp.)

#### Refraction

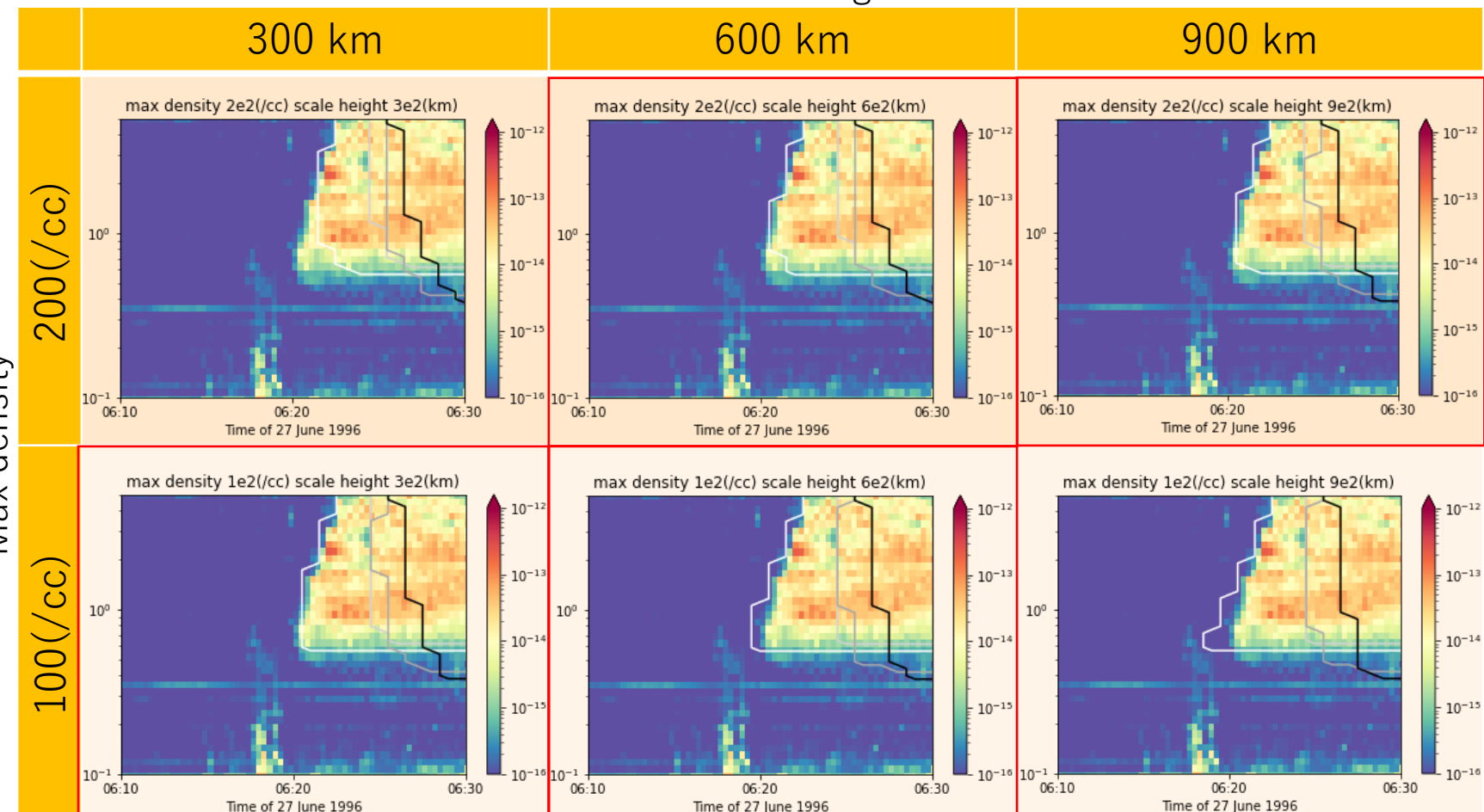


Fig.17 Superimposed Galileo PWS data and our results, assuming hydrostatic equilibrium plasma  
[ Max density : 200 • 100 (/cc) Scale height : 300 • 150 (km) ]

## 3-2. Ganymede ionosphere result

### Focus on egress

#### No refraction

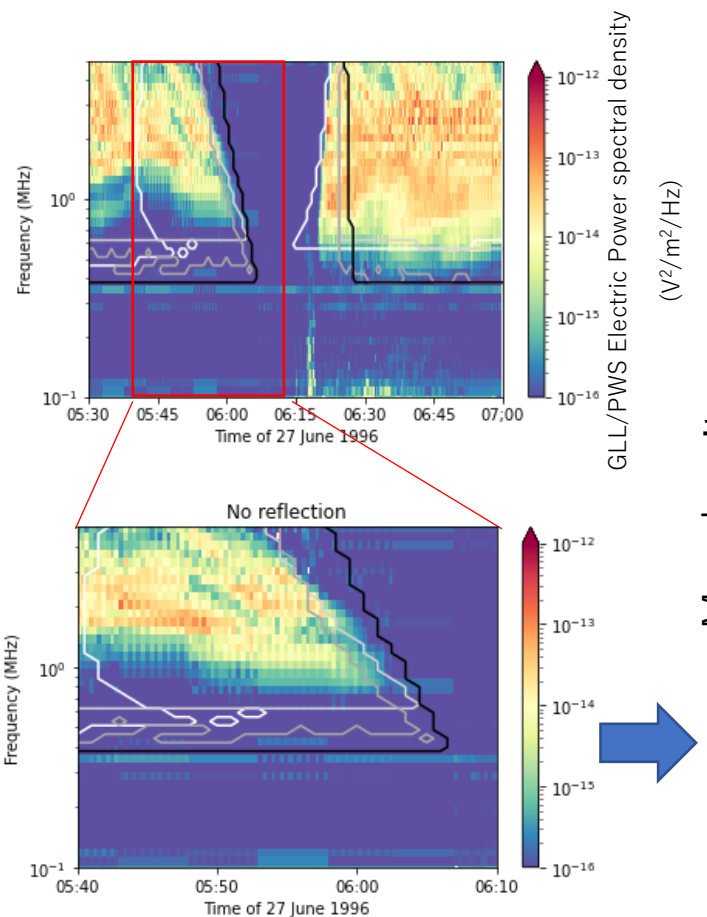


Fig.18 Superimposed Galileo PWS data and ExPRES simulations during Jovian radio emission occultations' egress by Ganymede . The four types of emission (A, B, C, D) are separated (from white to darkgrey, resp.)

#### Refraction

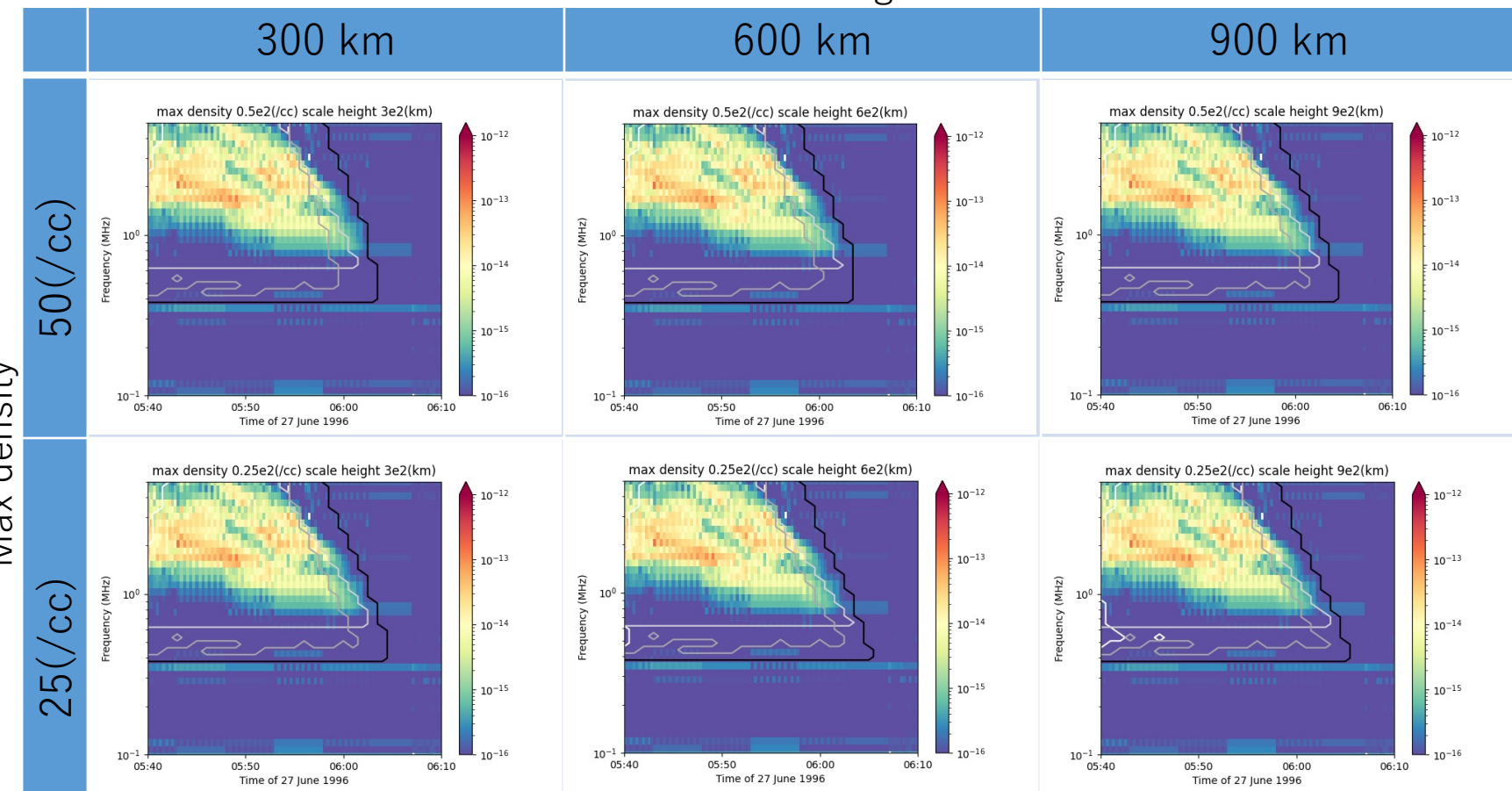


Fig.19 Superimposed Galileo PWS data and our results, assuming hydrostatic equilibrium plasma  
[ Max density : 50 · 25 (/cc) Scale height : 300 · 150 (km) ]

#### To discuss more quantitatively ...

1. Check radio intensity and the number.
2. Make histogram of the intensity. (Fig. 20)
3. Determine the threshold value [ $10e-15(V^2 / m^2 / Hz)$ ]
4. Determine ingress and egress timings.
5. Calculate average of the difference between the timing and our simulation result for each frequency.

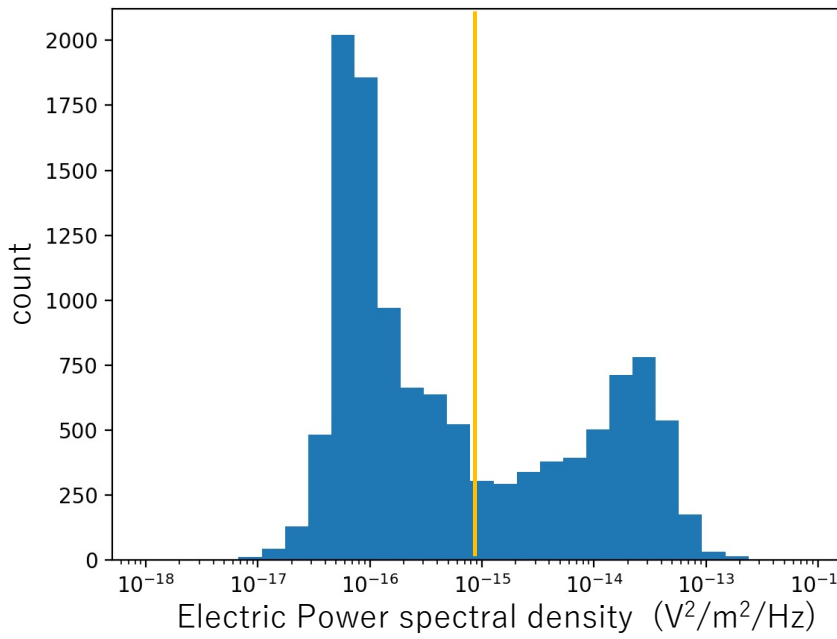


Fig.20 Histogram of the Galileo PWS data intensity

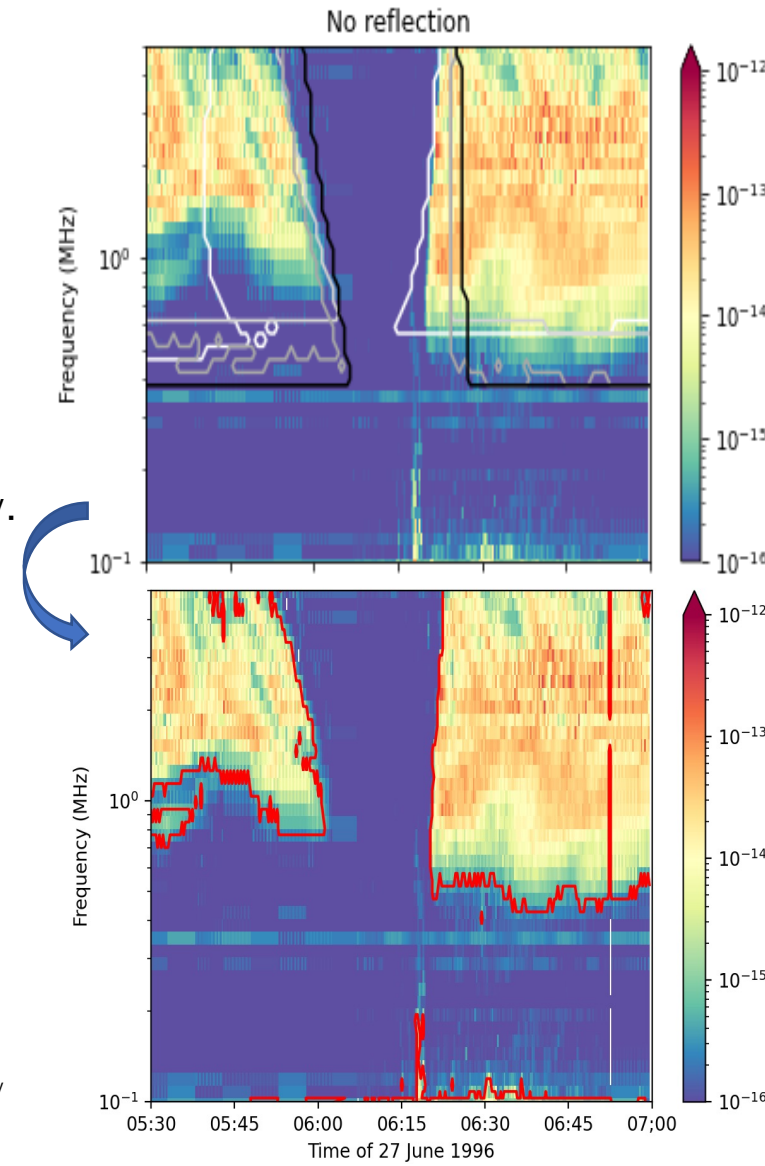


Fig.10 Superimposed Galileo PWS data and ExPRES simulations during Jovian radio emission occultations by Ganymede . The four types of emission (A, B, C, D) are separated (from white to darkgrey, resp.) [Cecconi et al, 2021]

Fig.21 Superimposed Galileo PWS data and boundary between detectable radio and ingress and egress timings.

### 3-3. Discussion

17

#### Focus on ingress

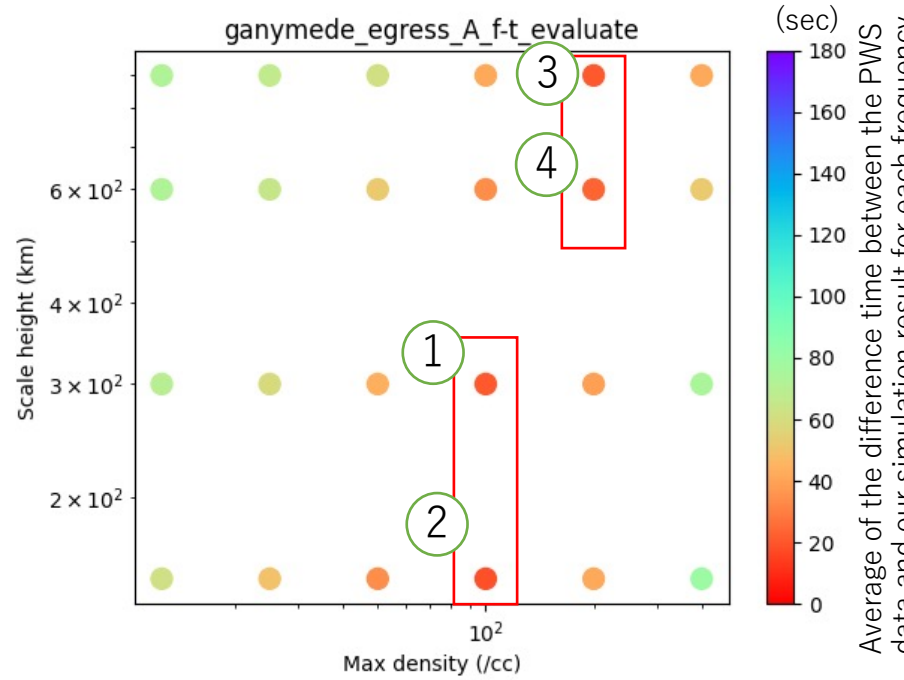


Fig.22 Average of the difference between ingress timing and our simulation result for each frequency, assumed max density and scale height of ionosphere distribution

#### Electron density distribution

- Scale height 150 (km) - Max 100 (/cc)
- Scale height 300 (km) - Max 100 (/cc)
- Scale height 600 (km) - Max 200 (/cc)
- Scale height 900 (km) - Max 200 (/cc)

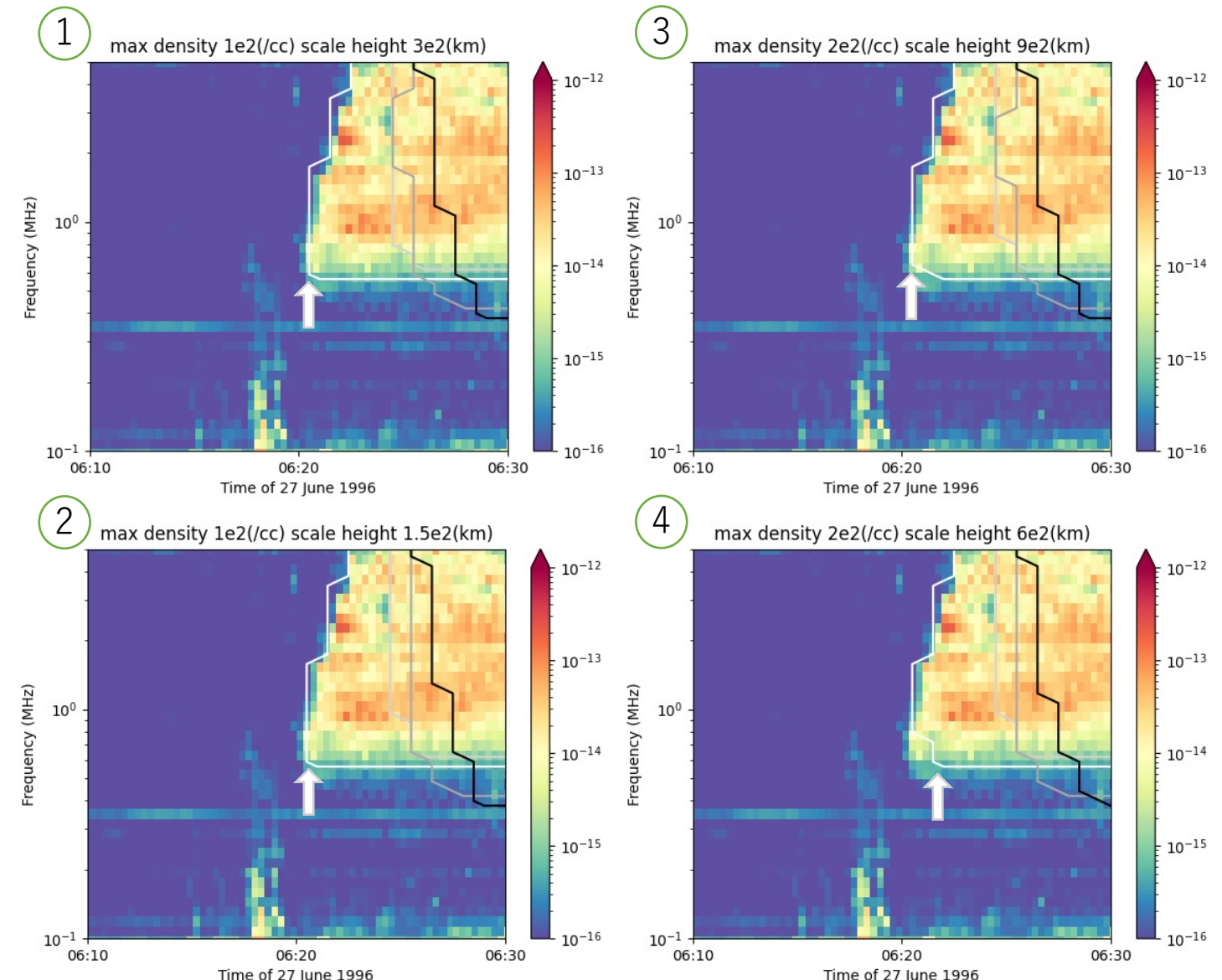


Fig.23 Superimposed Galileo PWS data and our results, assuming hydrostatic equilibrium plasma  
[ Max density and Scale height :  $100$  (/cc) &  $300$  (km) /  $100$  (/cc) &  $150$  (km) /  $200$  (/cc) &  $900$  (km) /  $200$  (/cc) &  $600$  (km) ]

### 3-3. Discussion

18

#### Focus on egress

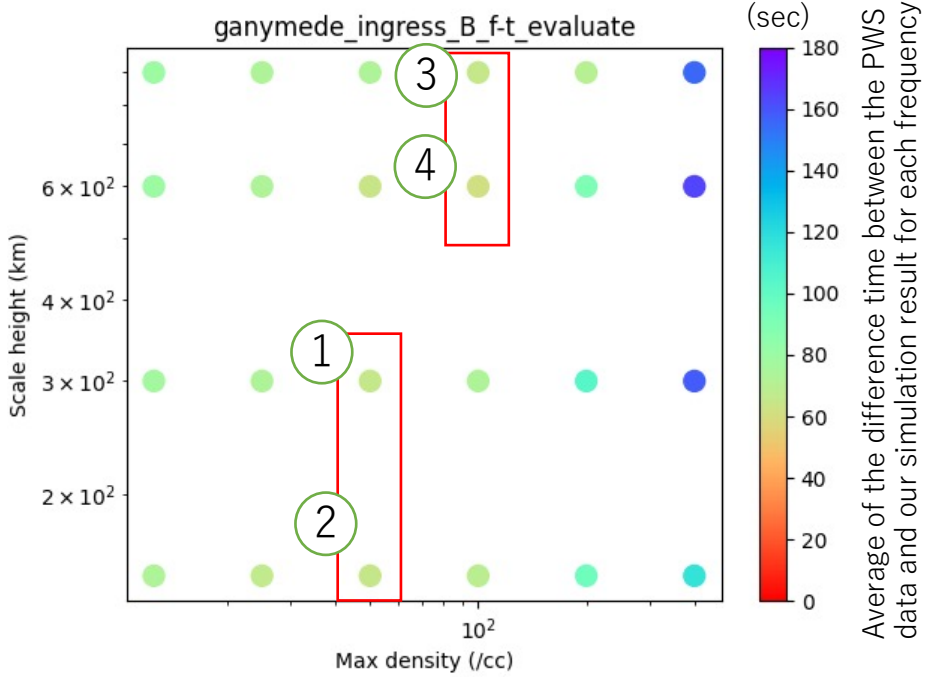


Fig.24 Average of the difference between egress timing and our simulation result for each frequency, assumed max density and scale height of ionosphere distribution

#### Electron density distribution

- Scale height 150 (km) - Max 50 (/cc)
- Scale height 300 (km) - Max 50 (/cc)
- Scale height 600 (km) - Max 100 (/cc)
- Scale height 900 (km) - Max 100 (/cc)

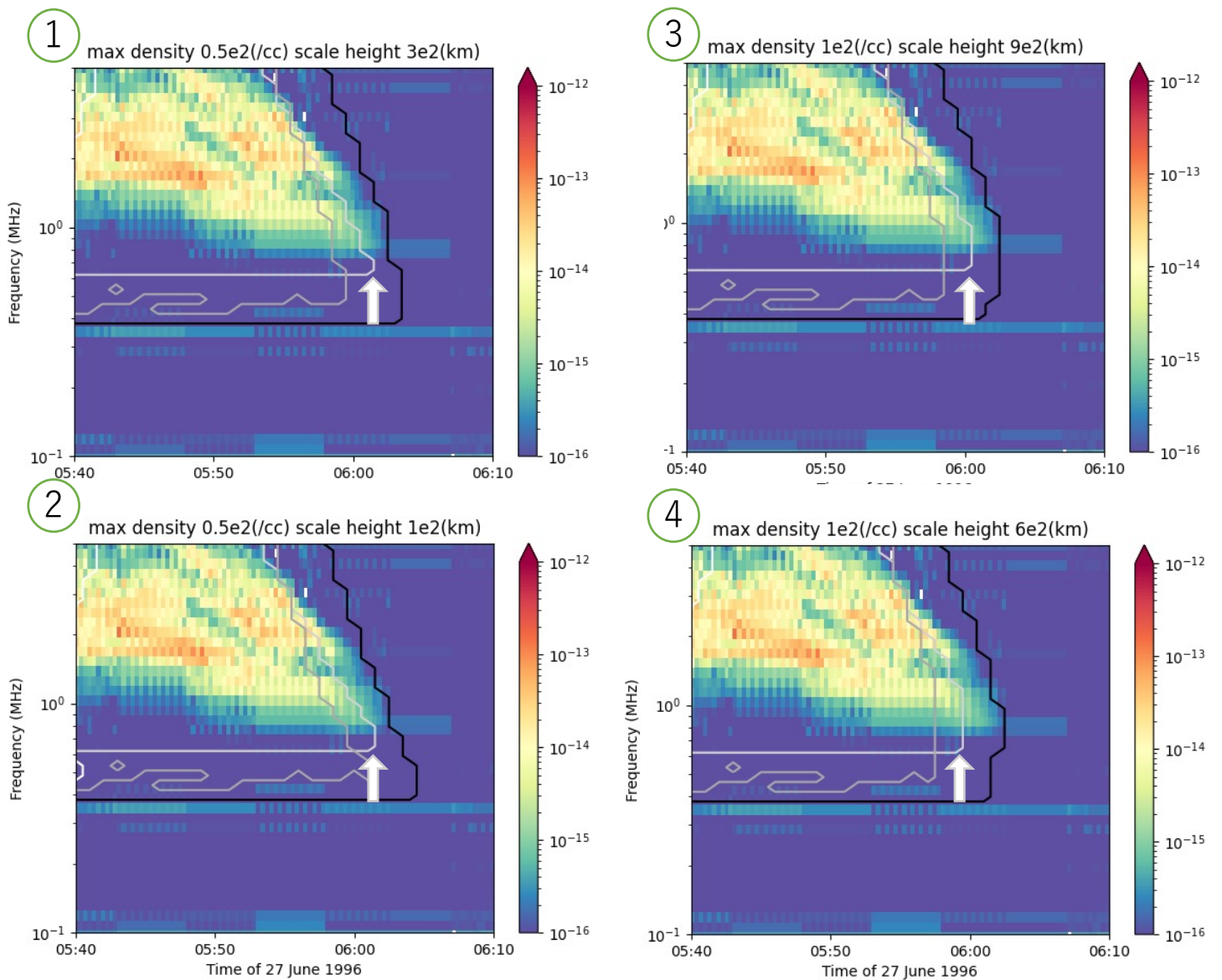


Fig.25 Superimposed Galileo PWS data and our results, assuming hydrostatic equilibrium plasma  
[ Max density and Scale height : 50(/cc) & 300(km) / 50(/cc) & 100(km) / 100(/cc) & 900(km) / 100(/cc) & 600(km) ]

### 3-3. Discussion

#### In-situ observation [Galileo PWS] and our results

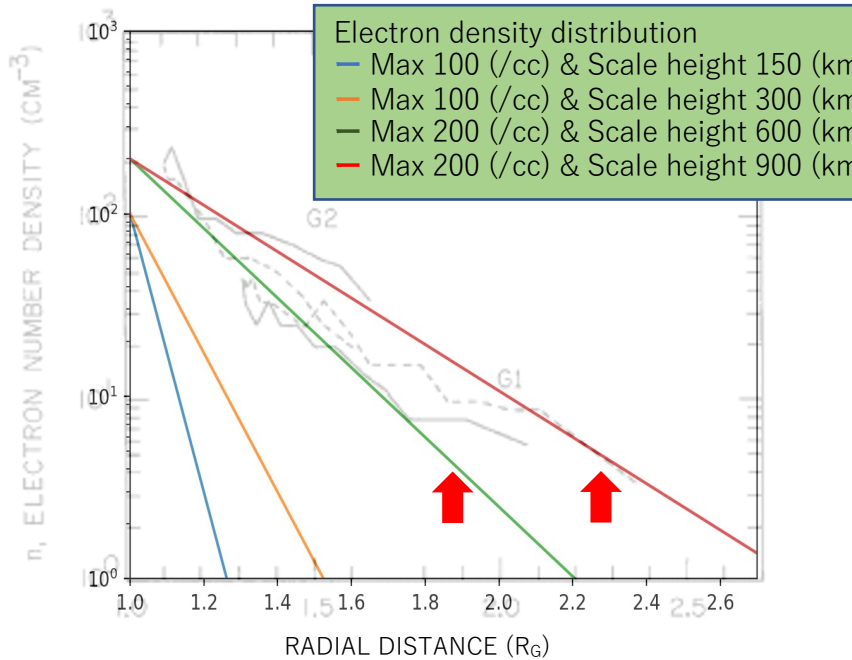


Fig.6 Electron density profiles on Ganymede 2 obtained by means of the PWS instrument on Galileo [Eviatar et al, 2001] and Electron density distribution during Ganymede G1 flyby that we estimate

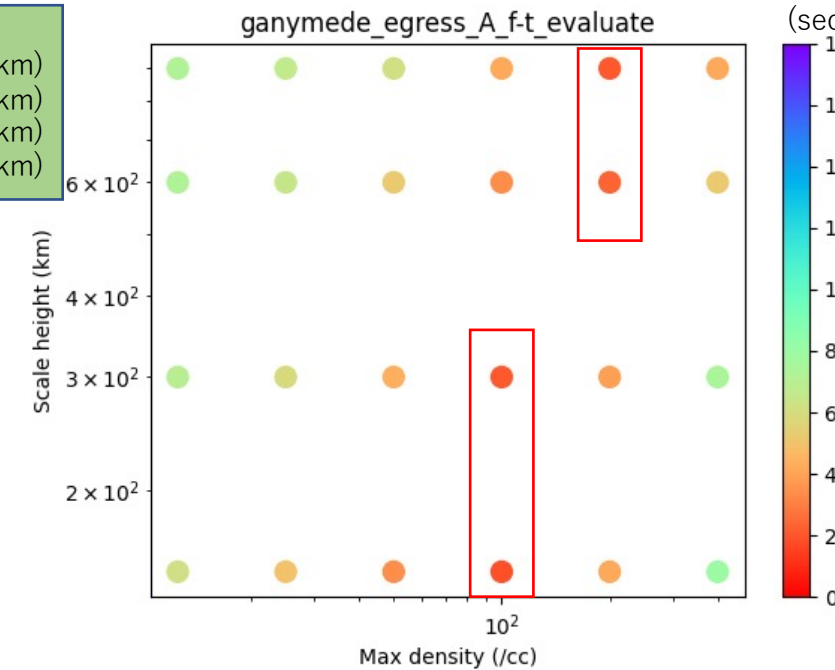
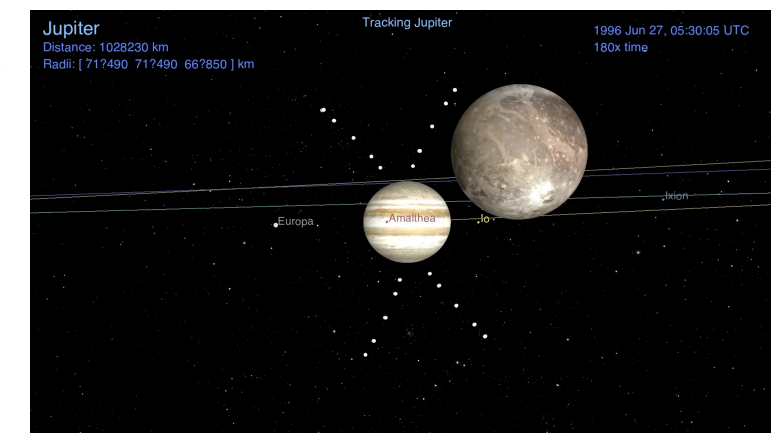


Fig.16 Superimposed Galileo PWS data and ExPRES simulations during Jovian radio emission occultations' egress by Ganymede . The four types of emission (A, B, C, D) are separated (from white to darkgrey, resp.)



- Some of our results (ex. red and green lines in Fig.15) match the In-situ observation results!
- Our results have strong sensitivity to maximum electron density.

In combination with In-situ observation, we can estimate the structure of the ionosphere.

### [Background]

- Structures of the interior, ionosphere and plume of the icy moons are essential information for understanding universality of habitable environment.

### [Purpose]

- Developing the numerical simulation code for the radar explorations using natural radio waves to investigate spatial structures of ionosphere and plumes created from the water oceanic materials.
- Finally, we will also investigate spatial structures of the interior.

### [Result]

- Hydrostatic equilibrium plasma ionosphere model can explain the Galileo PWS data during Jovian radio emission occultations.

### [Discussion]

- Some of our results (ex. red and green lines in Fig.15) match the In-situ observation results!
- In combination with In-situ observation, we can estimate the structure of the ionosphere.

- Aharon Eviatar, Vytenis M. Vasyliūnas, Donald A. Gurnett (2001), The ionosphere of Ganymede, Planetary and Space Science Volume 49, Issues 3–4, March 2001, Pages 327-336
- A. J. Kliore, D. P. Hinson, F. M. Flasar, A. F. Nagy, T. E. Cravens (1997), The Ionosphere of Europa from Galileo Radio Occultations, *Science* 18 Jul 1997: Vol. 277, Issue 5324, pp. 355-358 DOI: 10.1126/science.277.5324.355
- A. J. Kliore (1998), Satellite Atmospheres and Magnetospheres, DOI: <https://doi.org/10.1017/S1539299600019602>
- Kliore, A. J., Anabtawi, A, Nagy, A. F. ; Galileo Radio Propagation Science Team (2001b), The ionospheres of Ganymede and Callisto from Galileo radio occultations, *Bulletin of the American Astronomical Society*, Vol. 33, p.1084
- B. Cecconi, C. K. Louis, C. Muñoz Crego, and C. Vallat (2021), Auroral Radio Source Occultation Modeling and Application to the JUICE Science Mission Planning
- Kazuo Ouchi (2017), Principles of Radar - From Search Radar to Synthetic Aperture Radar, Publisher: Corona Publishing Co.
- Khurana, K., Kivelson, M., Stevenson, D. *et al.* Induced magnetic fields as evidence for subsurface oceans in Europa and Callisto. *Nature* 395, 777–780 (1998).
- Kimura, T., F. Tsuchiya, H. Misawa, A. Morioka, and H. Nozawa (2008a), Occurrence and source characteristics of the high - latitude components of Jovian broadband kilometric radiation, *Planet. Space Sci.*, **56**, 1155– 1168, doi:[10.1016/j.pss.2008.03.001](https://doi.org/10.1016/j.pss.2008.03.001).
- M.G. Kivelson, K.K. Khurana, M. Volwerk (2002), The permanent and inductive magnetic moments of Ganymede, *Icarus*, 157, pp. 507-522
- Paterson, W. R, Frank, L. A, Ackerson, K. L (1997), Galileo plasma observations at Europa: Ion energy spectra and moments, *Journal of Geophysical Research*, Volume 104, Issue A10, p. 22779-22792, doi:10.1029/1999JA900191
- Schubert et al. (2004). Interior, composition, structure and dynamics of the Galilean satellites, in Jupiter. The planet, satellites and magnetosphere, Cambridge University Press
- Xianzhe Jia, Margaret G. Kivelson, Krishan K. Khurana and William S. Kurth (2018), Evidence of a plume on Europa from Galileo magnetic and plasma wave signatures, *Nature Astronomy* 2, 459-464 (2018), DOI: 10.1038/s41550-018-0450-z
- MASER HP <https://maser.lesia.obspm.fr/publications/doi/auroral-radio-source-occultation.html?lang=en#G01> (2021/5/2)
- NASA HP <https://www.nasa.gov/topics/solarsystem/features/pia16826.html> (2021/5/2)
- GCOE HP <https://www.gcoe-earths.org/en/jupiter.html> (2021/5/2)